DOI 10.1007/s10812-017-0469-4
Journal of Applied Spectroscopy, Vol. 84, No. 2, May, 2017 (Russian Original Vol. 84, No. 2, March–April, 2017)

APPLICATION OF RAMAN SPECTROSCOPY FOR ANALYZING DIAMOND COATINGS ON A HARD ALLOY

A. A. Khomich,[a,b*] E. E. Ashkinazi,[a,c] V. G. Ralchenko,[a,c,d] V. S. Sedov,[a,c] R. A. Khmelnitskii,[b,e] O. N. Poklonskaya,[f] M. V. Kozlova,[g] and A. V. Khomich[a,b,c]

UDC 535.375.5; 549.211; 621.793.16

Single- and multilayer coatings of micro- and nanocrystalline diamond were deposited on tungsten carbide substrates (WC + 6 wt.% Co alloy) in a microwave plasma of methane/hydrogen and methane/hydrogen/nitrogen mixtures. Barrier tungsten layers were used to improve adhesion of the diamond coatings to the substrates. Raman spectroscopy was used to study the properties of the nano- and microcrystalline diamond coatings depending on the deposition parameters. Data on structural transformations of the coatings under different tribological contact conditions were obtained, and secondary nucleation processes were investigated on different diamond faces during the deposition from the gas phase.

Keywords: *diamond, vapor deposition, microwave plasma-chemical reactor, micro- and nanocrystalline films, Raman scattering, photoluminescence, friction, surface destruction.*

Introduction. Diamond coatings (DC) produced by chemical vapor deposition (CVD) on tungsten carbide substrates WC + 6 wt.% Co (WC6) many times increase the wear resistance and durability of carbide tools, significantly reduce the friction coefficient between chips and coating, prevent erosion and corrosion of the tool, reduce heat and build-up, and also improve the quality of the treated surface [1]. This is especially true for high-precision processing of metal-matrix and carbon-filled plastic composite materials for use in the aerospace, defense and nuclear industries. Increased adhesion to the substrate and improved cutting properties of the tool can be achieved by forming two- and multilayer DCs. Previous publications on the deposition and properties of two-layer micro/nanocrystalline composite DCs (e.g., see [1–4]) describe deposition of a nanocrystalline diamond layer from above. With this coating configuration, high hardness and good adhesion to the substrate of microcrystalline diamond layers [5] can be used together with low roughness and high elasticity of nanocrystalline diamond layers [3]. The use of multilayer DCs additionally helps to prevent cracking and increase their thermal conductivity [6].

Raman scattering is characterized by high sensitivity and spatial locality for a wide class of carbon compounds and allows obtaining data on their structure, composition, local stresses and basic impurities [7]. The correlation between the structure of DCs at the micro- and macrolevel, mechanisms of wear and surface failure and experimental Raman measurements data collected at various stages of deposition and testing of single- and multilayer DC is explored in this work. Electron microscopy and Raman scattering were used to study the deposition of diamond layers on different faces of diamond single crystals, which simulate the growth of nanocrystalline DC in multilayer structures on substrates of hard WC6 alloy.

Experiment. The synthesis of DC on WC6 and diamond substrates was carried out using a plasma-chemical microwave reactor ARDIS-100 from "Optosistemy" LLC (2.45 GHz, 5 kW). DCs were obtained by CVD in CH_4/H_2 and $CH_4/H_2/N_2$ mixtures by decomposing a carbon (methane) carrier in the plasma of the microwave reactor to form atomic hydrogen H and active CH_x radicals. The use of plasma contour as the main source of heat transfer by radiation made it

*To whom correspondence should be addressed.

[a]A. M. Prokhorov General Physics Institute, Russian Academy of Sciences, 38 Vavilov Str., Moscow, 119991, Russia; e-mail: antares-610@yandex.ru; [b]V. A. Kotelnikov Institute of Radio Engineering and Electronics, Russian Academy of Sciences, Fryazino Moscow region, Russia; [c]National Research Nuclear University MEPhI, Moscow, Russia; [d]Harbin Institute of Technology, Harbin, China; [e]P. N. Lebedev Physical Institute, Russian Academy of Sciences, Moscow, Russia; [f]Belarusian State University, Minsk, Belarus; [g]M. V. Lomonosov Moscow State University, Moscow, Russia. Translated from Zhurnal Prikladnoi Spektroskopii, Vol. 84, No. 2, pp. 295–302, March–April, 2017. Original article submitted November 16, 2016.

possible to realize for the first time in the plasma microwave reactor the method of group growth of DC on high-aspect plates of WC6 of arbitrary shape [8, 9]. The substrate temperature in the optimal range for the synthesis process is 740–760°C.

One of the fundamental problems in the deposition of DCs on substrates of the hard alloy WC6 is the catalytic effect of cobalt in the alloy leading to the formation of sp^2-carbon instead of diamond in the case of CVD. Cobalt was removed from the surface of the hard alloy substrates by the method of stage-by-stage chemical treatment of the substrate with Murakami′s reagent and Caro′s acid [9, 10]. To improve adhesion and block cobalt by magnetron sputtering, barrier layers of tungsten were formed according to the method described in [9]. Before the deposition of the DC on the intermediate layer of tungsten, detonation diamond and crushed synthetic diamond powders (with particle sizes of 5 and 50 nm) were applied to stimulate the nucleation of diamond, which ensured a density of diamond nuclei of ~10^9 particles/cm^3.

The structure, composition, and local stresses were studied by Raman spectroscopy and photoluminescence (PL) using a LabRam HR800 spectrometer (Horiba Jobin-Yvon) in a confocal configuration equipped with 1800 and 600 g/mm diffraction gratings. The spectral resolution for the 1800 g/mm grating was 2.0 cm^{-1}, the dispersion was 0.59 cm^{-1} with a slit width of 100 μm. The radiation from the excitation laser (λ = 473 nm) was collected in a backscattering geometry using an Olympus microscope objective lens (100×, numerical aperture NA = 0.90) with a spatial resolution of ~1 μm. The mapping of Raman spectra was carried out with the help of a motorized table Märzhäuser Wetzlar with a positioning accuracy of ~0.5 μm. To investigate the adhesion of coatings, the standard Rockwell method (hardness tester KB 3000) was used. The coefficient of friction was determined by measuring slip (Tribometer, CSM Instruments). The morphology of the DC surface was examined using a scanning electron microscope JSM-7001F.

Results and Discussion. *Investigation of degradation processes of single-layer DC in tribological tests.* Samples of single-layer micro- and nanocrystalline DCs on WC6 substrates with a diameter of 10 mm and a height of 4.5 mm were obtained by the CVD method in a plasma-chemical microwave reactor in methane–hydrogen mixtures. Synthesis of DC was carried out under the following conditions: microwave power 2.5–2.9 kW, pressure in the reactor chamber 10 kPa, gas mixture H_2/CH_4, methane concentration 4 and 15% for the growth of micro- and nanocrystalline DC. According to the scanning electron microscopy (SEM) results, microcrystalline DCs consist of 500–1000 nm grains with the preferential orientation (111) (Fig. 1a). No significant twinning of crystallites or defects related to unevenness of seeding on substrates was revealed. Nanocrystalline DCs consist primarily of randomly oriented grains <100 nm in size (Fig. 1b). The *HRc* hardness determined by the Rockwell test at different distances from the edge of the substrate for micro- and nanocrystalline DCs was 80.1 ± 0.5 and 80.4 ± 0.3 *HRc* units, respectively. Coefficients of friction when paired with a counterbody of Si_3N_4 (applied load 2 N, ball diameter 3 mm, rotation speed 5 cm/s) were 0.065 and 0.080 for nano- and microcrystalline DC, respectively [9].

Figure 2 shows the changes in Raman spectra of a nanocrystalline DC observed with increasing wear in experiments with a Si_3N_4-ball. According to the results of Raman spectroscopy, the initial DC is fairly homogeneous and is in a contracted state because of the difference in the coefficients of thermal expansion of the DC and the WC6 substrate. The peak maximum of the diamond Raman band is shifted from the normal position of 1332.5 to 1335 cm^{-1}, which corresponds to a compressive stress σ ~ 1.4 GPa. Its width at half-maximum is $\Gamma_{1/2}$ = 9 cm^{-1}. The compressive stress σ was calculated from the shift of the diamond band Δμ in the Raman spectrum using the ratio σ = –0.57Δμ [11]. In addition to the diamond peak, the following bands can be found in Raman spectra: *D* (1350 cm^{-1}, $\Gamma_{1/2} \approx 40$ cm^{-1}) and *G* (1605 cm^{-1}, $\Gamma_{1/2} \approx 80$ cm^{-1}) bands that are due to the disordered non-diamond sp^2-carbon, and bands at 1145 and 1475 cm^{-1} due to vibrations of hydrocarbon trans-polyacetylene (TPA) chains at the intercrystalline boundaries characteristic for nanocrystalline DC [12]. Due to elastic stresses, intercrystalline boundaries and local inhomogeneities of the structure, half-widths and the positions of the band maxima in the Raman spectra vary along the DC surface within 5 cm^{-1}. With increasing wear, decreasing amplitude and broadening of the diamond peak and a significant decrease in the intensities of the bands at 1145 and 1475 cm^{-1} (spectrum *2*) occur successively, and the ratio of intensities of the *D* and *G* bands varies insignificantly. At the same time, the position of the bands changes. The shift of the TPA chain bands and the *D* band to lower frequencies can be explained by the disordering of the length of the chains [12] and the ordering of sp^2-hybridized C=C bonds in aromatic rings [12]. Such changes in the Raman spectra do not contradict the theoretical notions [13] and microscopic data [14] on the structural rearrangement of nanocrystalline DCs undergoing tribological tests. According to [13, 14], the plastic deformation of the near-surface layer at the areas of contact with the ball leads to amorphization not only of the near-surface layer of the DC, but also the ~100 nm thick transitional layer located below. In addition, wear products provide the formation of a solid lubricant layer on the surface of the DC. The surface energy on the wear track is higher compared to the surface of the film. An increase in the concentration of defects in the near-surface layer of the DC, including dangling carbon bonds, leads to an increase in chemical activity [15],

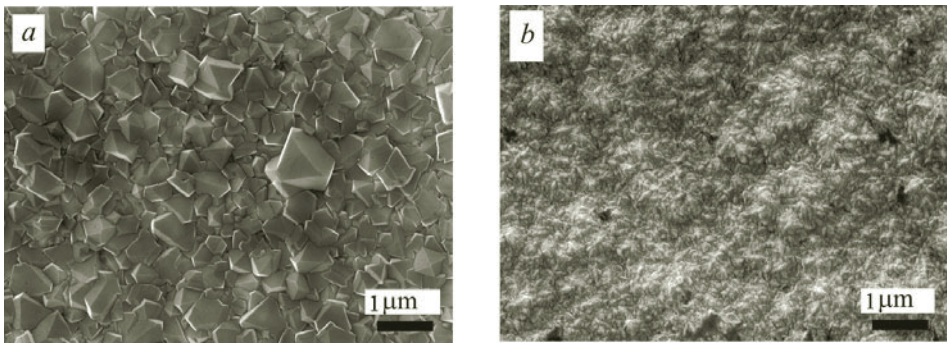

Fig. 1. SEM images (15,000×) of diamond coatings deposited at a 4% (microcrystalline DC) (*a*) and 15% (nanocrystalline DC) (*b*) concentration of methane in the gas mixture.

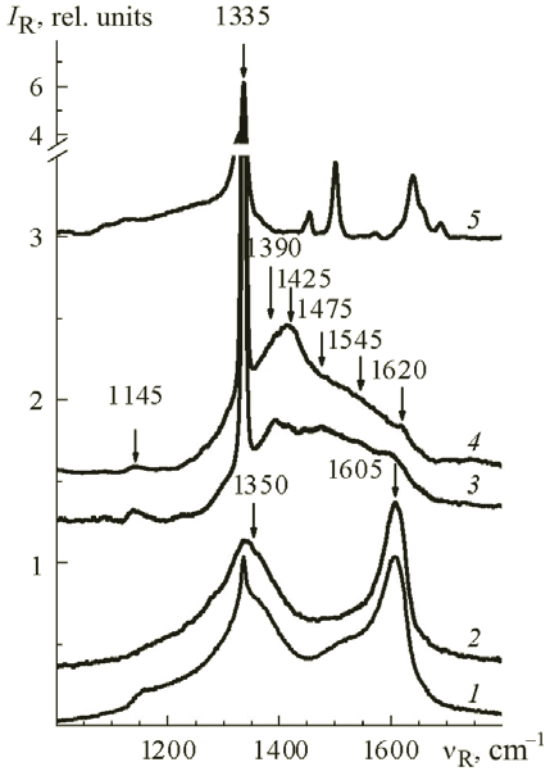

Fig. 2. Raman spectra of single-layer nano- and microcrystalline DC measured in the undamaged region (1 and 3) and in the region of maximum wear (2 and 4) after tribological tests with a Si_3N_4 counter-ball; 5) spectrum of a natural diamond crystal implanted with nickel ions [22]; the spectra are shifted vertically relative to each other for clarity.

which in turn reduces the coefficient of friction [16]. The stepwise nature of the transformation of Raman spectra is in good agreement with the nonmonotonicity of the change in the friction coefficient of the same sample during the tests [9].

In the Raman spectra of microcrystalline DC (Fig. 2), a diamond peak ($\Gamma_{1/2}$ = 6 cm^{-1}) with a maximum at $\Delta\nu_R$ = 1335 cm^{-1} is dominant. In addition to low-intensity Raman bands with maxima at 1155, 1350, and 1475 cm^{-1} observed in the spectra of nanocrystalline DCs, relatively narrow ($\Gamma_{1/2}$ = 20–30 cm^{-1}) bands with maxima near 1390, 1425, and 1620 cm^{-1} (spectra 3 and 4) appear in the Raman spectra of microcrystalline DCs. The relative intensity of these bands varies along the surface of the DC probably determined by the morphological features of the coating composed of ~0.5–5 μm diamond

crystallites, i.e., combining the properties of nano- and microcrystalline DCs. The band near 1620 cm^{-1} in the Raman spectra of DC may indicate the presence of microcrystalline graphite inclusions [12, 16]. After tribological tests, the diamond peak widened to $\Gamma_{1/2}$ = 9 cm^{-1}, the 1145 cm^{-1} band slightly weakened and shifted to lower frequencies, and the band with a maximum near 1425 cm^{-1} (spectrum *4*), which according to [13] is due to diamond lattice defects in the twinning regions, significantly increased. No Raman bands characteristic of the Si_3N_4 counterbody material were observed.

The nature of additional relatively narrow (20–30 cm^{-1} wide at half-maximum) bands in the spectra of microcrystalline DCs in the range of 1350–1550 cm^{-1} is still under discussion. Such a high frequency is not characteristic for any form of sp^3-carbon, for which the maximum possible frequency of oscillation is ~1400 cm^{-1} [17]. Bands close in position and widths at half-maximum were observed, for example, in the Raman spectra of microcrystalline DCs deposited from various gas mixtures by the hot-filament method on WC6 substrates [18], and also in [19], but their nature was not discussed. In the Raman spectra of diamonds subjected to ion-implantation or fast neutron irradiation [20–23] several relatively narrow bands due to vibrations of complexes of intrinsic defects in the diamond lattice were observed in the 1400–1800 cm^{-1} range. Discrepancies of Raman frequencies at 1390 and 1425 cm^{-1} between the spectra of microcrystalline DCs on WC6 (Fig. 2) and the spectra of radiation-damaged diamonds support the theory that these two bands are due to defects found not in the bulk of the diamond crystallites, but at the intercrystalline boundaries and in the twinning regions in DC on WC6, in particular, regions of conjugated sp^2-carbon chains [24].

Investigation of the profile of two-layer DC by means of Raman spectroscopy. Confocal Raman spectroscopy is effective for investigating the profile of DC [4], in which the lower microcrystalline layer has high hardness, elasticity and good adhesion to the WC6 substrate, and the upper nanocrystalline layer has high bending strength, low roughness and a low coefficient of friction. At present, two-layer DC on WC6-substrates are deposited by the "hot filament" method, and grain size is controlled either through bias voltage [6, 25] or changes in methane concentration and the pressure of the mixture [4].

In the present work, formation of the structure of DC layers was controlled by adding nitrogen to the microwave reactor, which causes secondary nucleation and a decrease in the size of diamond crystallites [26, 27]. Multi-sided 12.5 × 12.5 × 3.5 mm cutting plates of WC6 with a back angle of 11^o (GOST 19064-80) were used as the carbide substrates. DC were deposited for 5 h at 750^oC: in a CH_4/H_2 mixture for the first 2.5 h, then N_2 was added, and its concentration to the total gas flow was maintained at 4%, since an increase in nitrogen concentration of <10% markedly reduces the hardness of the deposited nanocrystalline DC [28]. Samples for measuring the Raman spectra were separated from the WC6 substrate as a result of the Rockwell DC adhesion testing. The laser spot size during scanning was 1 μm, the scanning step was 0.5 μm.

Figure 3 shows the Raman spectra in four characteristic regions along the thickness of the DC. There are five bands of variable intensity. The maximum of the diamond Raman peak ($\Gamma_{1/2}$ varies from 10 to 20 cm^{-1}) is at 1332–1333 cm^{-1}. In addition to the diamond peak, the following bands are observed: *D* (1350 cm^{-1}) and *G* (1560 cm^{-1}) bands due to disordered non-diamond sp^2-carbon, and the bands at 1140 and 1490 cm^{-1} characteristic for nanocrystalline DCs and occurring due to oscillations of the TPA chains at intercrystalline boundaries. The ratio between the intensities of the bands varies along the thickness of the DC reflecting the changes in its structure. At the beginning of the deposition process, diamond layers with Raman spectra characteristic of nanocrystalline diamond (spectrum *1*) are formed. With further deposition of the DC, at the DC thickness of ~1–1.5 μm the $G_{1/2}$ of the diamond peak and the intensity of the bands characteristic of TPA chains located at intercrystallite boundaries decrease both relative to the diamond peak (spectrum *2*) and the *G* band. The addition of nitrogen to the microwave reactor causes secondary nucleation processes with a decrease in the crystallite size. The region of transition from micro- to nanocrystalline DC is well defined in the Raman spectra (Fig. 3) by broadening and decrease of the relative intensity of the diamond band with a maximum near 1332 cm^{-1}, and also by intensification of the Raman bands of TPA chains. The region of transition from micro- to nanocrystalline growth is 5 microns from the WC6 substrate. From this value the average deposition rates of nano- and microcrystalline diamond were estimated at 50 and 30 nm/min, respectively.

When changing the DC deposition regime, it is important to prevent the formation of a layer with a high concentration of sp^2-carbons at the interface [4, 6] and simultaneously ensure the formation of a smooth and durable DC. Judging from the Raman spectroscopy data, after the addition of nitrogen during CVD in a microwave reactor, an ~2 micron thick transition layer is formed that combines the properties of micro- and nanocrystalline DCs, which, according to [1, 4, 6], increases the resistance of DC on WC6 to extreme mechanical and thermal stresses. The formation of a 1–1.5-μm-thick layer of nanocrystalline diamond near the nucleation side did not negatively impact adhesion, hardness (85 *HRc* units), and wear resistance of the two-layer DC.

Attempts to form a wear track on the surface of the DC in the action region of a Si_3N_4 ball counterbody at a load of 1 N failed. Wear of the DC did not exceed $1.5 \cdot 10^{-4}$ $\mu m^3/(N \cdot m)$, which is almost four orders of magnitude lower than the

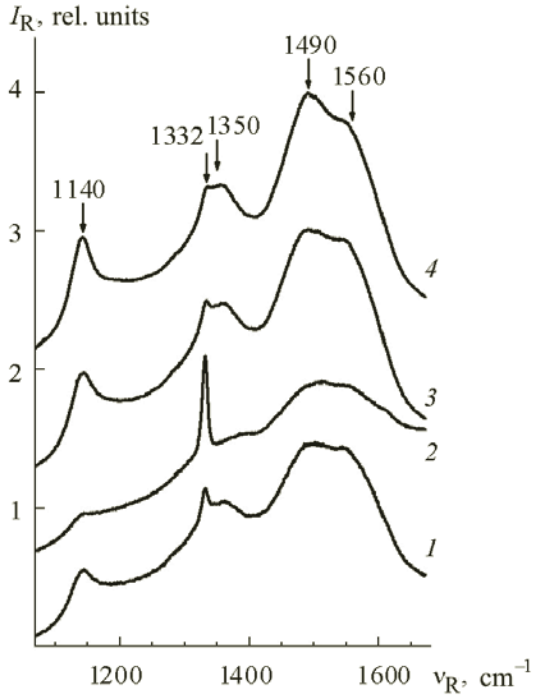

Fig. 3 Changes of the Raman spectrum measured across the cleavage of a two-layer DC deposited in a microwave reactor: 1) near the WC6 substrate, 2) microcrystalline DC layer (4 μm from the nucleation side), 3) nanocrystalline DC layer (7 μm from the nucleation side), 4) near the growth surface of the DC; the spectra are shifted vertically relative to each other.

reduced wear of the Si_3N_4 ball. The friction coefficient between the DC and Si_3N_4 is <0.06. Raman spectra on the surface of a nanocrystalline DC (Fig. 2, spectrum *4*) are not sensitive to the action of a Si_3N_4 ball. From these data, it appears that the addition of 4% nitrogen during CVD in a microwave reactor improves the mechanical properties of nanocrystalline DCs, as is the case with doping DC with silicon or boron [29] during CVD by the hot-filament method.

Growth of nanocrystalline diamond on various growth faces of a single-crystal diamond. When depositing the upper nanocrystalline layer in a two-layer DC on WC6, it is important to achieve a continuous smooth coating on the faceted microcrystalline film while avoiding the formation of an sp^2-layer in the interface region. To simulate the CVD of nanocrystalline DC on different crystallographic faces of a microcrystalline DC, a faceted single-crystal diamond was used as the substrate. The deposition of a DC on the diamond substrate was carried out in regimes close to the deposition of nanocrystalline DCs on WC6, namely, in a $H_2/CH_4/N_2$ gas mixture with a total gas flow rate of 500 std. cm^3/min (92% H_2/4% CH_4/4% N_2) under chamber pressure of 130 torr and 2.8 kW microwave power. As a substrate, a diamond crystal grown under high pressure and temperature gradient (HPHT) conditions was used; the upper part of the diamond containing {001}, {110}, {111}, {211}, and {311} was cut off along the (001) plane. The thickness of the diamond HPHT substrate was 0.9 mm, which ensures the closest growth conditions on its faces in the microwave reactor.

According to electron microscopy data, the morphology of the DC on the {100} and {111} substrate surfaces is different: the {100} faces are smooth and conducive to homoepitaxial diamond growth, while on the {111} and {110} faces a nanocrystalline DC forms with crystallites from several tens up to hundreds of nanometers in size. The original {311} and {211} faces of the substrate do not contain any areas yielding {100} crystalline planes, but already at the initial stage of growth clearly defined smooth sections of the {100} plane form on the tops of the {111} type layers. With further growth of these faces, the area of the {100} faces decreases and polycrystalline regions are formed on them.

At the end of the 5-min growth session, Raman spectra of the DCs deposited all the faces of the diamond sample were measured (Fig. 4). The Raman spectrum on the {100} face of the HPHT diamond substrate contains only the main diamond band ($\Delta\nu_R$ = 1332.5 cm^{-1}, $\Gamma_{1/2}$ = 2.7 cm^{-1}). On the other faces, the spectra also contain broad bands of disordered carbon with maxima at 1355 and 1560 cm^{-1} (*D* and *G* bands) and characteristic for nanocrystalline DC bands of TPA chains (with maxima

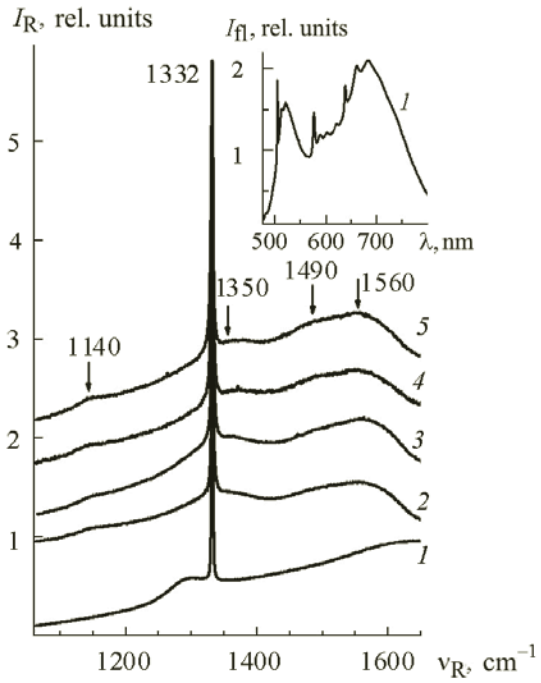

Fig. 4. Raman spectra of DC deposited for 5 min from the hydrogen/methane/nitrogen mixture on the {100} (1), {110} (2), {111} (3), {211} (4), and {311} (5) planes of a single-crystal diamond synthesized by the HPHT method; the spectra are displaced vertically relative to each other for clarity; on the inset — the PL spectrum measured on the {100} plane of the DC.

at 1140 and 1490 cm^{-1}) [11]. $\Gamma_{1/2}$ of the diamond Raman peak increases in order {100}→{110}→{111}→→{211}→{311} from 2.7 to 4.3 cm^{-1}. Its position for the {100} and {211} faces corresponds to the unstressed diamond; for the {111} and {110} faces, the displacement of the diamond peak corresponds to compressive stress of 0.15 GPa; for the {311} plane it corresponds to tensile strain of 0.3–0.6 GPa. The ratio of the intensities of the TPA chain bands and the *G*-band to the area of the diamond peak increases in order {100}→{211}→{111}≈{110}→{311} and {100}→{211}→{111}→{311 }≈{110}.

In the Raman spectrum of the {100} plane of the DC at the excitation wavelength of 473 nm there are no *G*, *D* and TPA bands, but a broad band with a maximum near 1300 cm^{-1} due to PL is observed (Fig. 4, inset). In addition to the bands with zero-phonon lines at 575 and 638 nm (NV^0 and NV^- centers), a band with a zero-phonon line at 503 nm (2NV center) is present in the PL spectrum of the {100} plane, which was previously observed in unirradiated CVD DCs only after high-temperature (1500^{o}C and higher) annealing in a vacuum [12, 30]. Its appearance in the PL spectra of the investigated DC indicates a high concentration of impurity nitrogen in DC due to the high mobility of nitrogen-containing radicals on the growth surface under CVD [31].

Conclusions. Very hard micro- and nanocrystalline single- and two-layer diamond coatings were deposited on WC6 hard alloy substrates in microwave plasma from methane–hydrogen mixtures, and a group growth regime was realized on high-aspect metal substrates. The relationship between the crystal structure and the tribological properties of thin diamond coatings deposited from CH_4/H_2 mixtures was investigated by Raman spectroscopy. It was found that the wear of nanocrystalline diamond coatings is associated with the processes of their amorphization, while the wear of more stable microcrystalline diamond coatings is associated with the accumulation of point and extended defects in the twinning regions and near intercrystalline boundaries. The addition of nitrogen to the gas phase makes it possible to deposit solid, smooth and wear-resistant two-layer micro/nanocrystalline diamond coatings in microwave plasma, the change in the structure of which can be traced in Raman spectra. The processes of deposition of nanocrystalline diamond coatings on various faces of a single-crystal diamond were studied by Raman spectroscopy and electron microscopy. It was found that in the deposition regimes close to those used for the deposition of diamond coatings on WC6 substrates homoepitaxial growth takes place on the {100} faces of the diamond, and a nanocrystalline diamond coating with crystallite sizes ranging

from several tens to hundreds of nanometers is deposited on the {111} and {110} faces, while on the {311} and {211} faces a mixed growth regime is realized.

Acknowledgments. The authors thank P. A. Tsygankov and D. N. Sovyk for preparing the WC6 substrates and M. I. Petrzhik for measuring the dynamic coefficient of friction. The work was supported by the Russian Science Foundation (project No. 15-19-00279).

REFERENCES

1. R. Dumpala, M. Chandran, and M. S. R. Rao, *JOM*, **67**, No. 7, 1565–1577 (2015).
2. S. A. Catledge, P. Baker, J. T. Tarvin, and Y. K. Vohra, *Diamond Relat. Mater.*, **9**, No. 7, 1512–1517 (2000).
3. F. Sun, Y. Ma, B. Shen, Z. Zhang, and M. Chen, *Diamond Relat. Mater.*, **18**, No. 2, 276–279 (2009).
4. R. Dumpala, B. Ramamoorthy, and M. S. R. Rao, *Appl. Surf. Sci.*, **289**, 545–550 (2014).
5. F. A. Almeida, M. Amaral, F. J. Oliveira, A. J. S. Fernandes, and R. F. Silva, *Vacuum*, **81**, No. 11, 1443–1447 (2007).
6. L. Shafer, M. Hofer, and R. Kroger, *Thin Solid Films*, **515**, No. 3, 1017–1024 (2006).
7. J. W. Ager and M. D. Drory, *Phys. Rev. B*, **48**, No. 4, 2601–2607 (1993).
8. E. E. Ashkinazi, V. S. Sedov, D. N. Sovyk, A. V. Khomich, V. G. Ral′chenko, P. A. Tsyganov, D. V. Vinogradov, and V. I. Konov, *Coll. Abstracts of the Reports of the 10th Int. Conf. "Carbon: Fundamental Problems of Science, Materials Science, Technology"* [in Russian], 6–9 June, 2016, Troitsk (2016), pp. 43–45.
9. E. E. Ashkinazi, V. S. Sedov, M. I. Petrzhik, D. N. Sovyk, A. A. Khomich, V. G. Ral′chenko, D. V. Vinogradov, P. A. Tsyganov, I. N. Ushakova, and A. V. Khomich, *Treniye Iznos*, **38**, No. 3, 280–288 (2017).
10. R. Polini, *Thin Solid Films*, **515**, No. 1, 4–13 (2006).
11. A. C. Ferrari and J. Robertson, *Phil. Trans. R. Soc. A*, **362**, No. 1824, 2477–2512 (2004).
12. A. M. Zaitsev, *Optical Properties of Diamond. A Data Handbook*, Springer, Berlin (2001).
13. L. Pastewka, S. Moser, P. Gumbsch, and M. Moseler, *Nature Mater.*, **10**, No. 1, 34–38 (2011).
14. X. Zhang, R. Schneider, E. M. Müller, S. Meier, P. Gumbsch, and D. Gerthsen, *J. Appl. Phys.*, **115**, No. 6, 063508 (2014).
15. X. Lei, B. Shen, S. Chen, L. Wang, and F. Sun, *Trib. Intern.*, **69**, 118–127 (2014).
16. R. B. Jackman, J. Beckman, and J. S. Foord, *Diamond Relat. Mater.*, **4**, No. 5–6, 735–739 (1995).
17. D. Hyde-Volpe, B. Slepetz, and M. Kertesz, *J. Phys. Chem. C*, **114**, No. 21, 9563–9567 (2010).
18. X. Wang, X. Shen, F. Sun, and B. Shen, *Tribol. Lett.*, **61**, No. 2 (2016); doi: 10.1007/s11249-015-0639-6.
19. R. Polini, M. Barletta, and G. Cristofanilli, *Thin Solid Films*, **519**, No. 5, 1629–1635 (2010).
20. S. Prawer, I. Rosenblum, J. O. Orwa, and J. Adler, *Chem. Phys. Lett.*, **390**, Nos. 4–6, 458–461 (2004).
21. A. V. Khomich, R. A. Khmelnitskii, X. J. Hu, A. A. Khomich, A. F. Popovich, I. I. Vlasov, V. A. Dravin, Y. G. Chen, A. E. Karkin, and V. G. Ralchenko, *Zh. Prikl. Spektrosk.*, **80**, No. 5, 719–726 (2013) [A. V. Khomich, R. A. Khmelnitskii, X. J. Hu, A. A. Khomich, A. F. Popovich, I. I. Vlasov, V. A. Dravin, Y. G. Chen, A. E. Karkin, and V. G. Ralchenko, *J. Appl. Spectrosc.*, **80**, 707–714 (2013)].
22. O. N. Poklonskaya and A. A. Khomich, *Zh. Prikl. Spektrosk.*, **80**, No. 5, 715–720 (2013)] [O. N. Poklonskaya and A. A. Khomich, *J. Appl. Spectrosc.*, **80**, 715–720 (2013)]
23. O. N. Poklonskaya, S. A. Vyrko, A. A. Khomich, A. A. Averin, A. V. Khomich, R. A. Khmelnitsky, and N. A. Poklonski, *Zh. Prikl. Spektrosk.*, **81**, No. 6, 879–887 (2014) [O. N. Poklonskaya, S. A. Vyrko, A. A. Khomich, A. A. Averin, A. V. Khomich, R. A. Khmelnitsky, and N. A. Poklonski, *J. Appl. Spectrosc.*, **81**, 969–977 (2014)].
24. M. Veres, M. Koós, S. Tóth, and L. Himics, *IOP Conf. Ser.: Mater. Sci. Eng.*, **15**, 012023 (2010).
25. S. Takeuchi, M. Kojima, S. Takano, K. Kazutaka, and M. Murakawa, *Thin Solid Films*, **469–470**, 190–193 (2004).
26. K. Subramanian, W. P. Kang, J. L. Davidson, and W. H. Hofmeister, *Diamond Relat. Mater.*, **14**, No. 1, 86–91 (2005).
27. V. Ralchenko, S. Pimenov, V. Konov, A. Khomich, A. Saveliev, A. Popovich, I. Vlasov, E. Zavedeev, A. Bozhko, E. Loubnin, and R. Khmelnitskii, *Diamond Relat. Mater.*, **16**, No. 12, 2067–2073 (2007).
28. S. A. Catledge, J. Borham, Y. K. Vohra, W. R. Lacefield, and J. E. Lemons, *J. Appl. Phys.*, **91**, No. 8, 5347–5352 (2002).
29. J. G. Zhang, X. C. Wang, B. Shen, and F. H. Sun, *Int. J. Refract. Met. Hard Mater.*, **41**, 285–292 (2013).
30. A. V. Inyushkin, A. N. Taldenkov, V. G. Ralchenko, I. I. Vlasov, V. I. Konov, A. V. Khomich, R. A. Khmelnitskii, and A. S. Trushin, *Phys. Status Solidi* (a), **205**, No. 9, 2226–2232 (2008).
31. H. Yamada, A. Chayahara, and Y. Mokuno, *Jpn. J. Appl. Phys.*, **55**, No. 1S, 01AC07 (2016).